NASA TECHNICAL NOTE

NASA TN D-3513

NASA TN D-3513

ATOMIZATION OF ETHANOL JETS IN A COMBUSTOR WITH OSCILLATORY COMBUSTION-GAS FLOW

by Robert D. Ingebo

Lewis Research Center
Cleveland, Ohio

NATIONAL AERONAUTICS AND SPACE ADMINISTRATION • WASHINGTON, D. C. • JULY 1966

NASA TN D-3513

ATOMIZATION OF ETHANOL JETS IN A COMBUSTOR WITH OSCILLATORY COMBUSTION-GAS FLOW

By Robert D. Ingebo

Lewis Research Center
Cleveland, Ohio

NATIONAL AERONAUTICS AND SPACE ADMINISTRATION

For sale by the Clearinghouse for Federal Scientific and Technical Information
Springfield, Virginia 22151 – Price $1.00

ATOMIZATION OF ETHANOL JETS IN A COMBUSTOR WITH OSCILLATORY COMBUSTION-GAS FLOW

by Robert D. Ingebo

Lewis Research Center

SUMMARY

Drop-size-distribution data were obtained for jets of ethanol atomized by downstream injection from a simple orifice into a combustion-gas stream inside a rocket combustor. High-frequency acoustic oscillations were induced in the combustor by a siren exhaust system. A high-speed camera was used to obtain photomicrographs of the ethanol sprays at several distances downstream from the injection-tube orifice and over a range of amplitude variations in the acoustic oscillations produced by the siren at a fixed frequency of 1190±5 cps. From the photomicrographs, the volume-number mean drop diameter D_{30} was calculated by direct integration of the drop-size data and compared with values of D_{30} obtained from the Nukiyama-Tanasawa expression for drop-size distribution. The results showed good agreement.

Fine atomization was obtained with the siren exhaust system in operation, D_{30} equals 62 microns; whereas, without the controlled oscillations, D_{30} was considerably larger, 217 microns. Also, the atomization process was more rapid with the siren operating. Complete breakup occurred 1 inch downstream from the injector-tube orifice, whereas without the controlled oscillations, 6 inches were required. Similarly, the distance required for relatively complete vaporization, with the 1190-cps oscillations, was 2 inches, whereas, without such oscillations, more than 2 feet were needed. Values of D_{30} determined under "resonant" combustion conditions, agreed fairly well with the following expression derived for crosscurrent breakup of liquid jets in airstreams: $D_{30}/D_o = 3.9(WbRe)^{-1/4}$. In this expression, $Wb = \rho_g D_o(\Delta V)^2/\sigma$, and $Re = D_o \Delta V/\nu$ where σ and ν are the surface tension and kinematic viscosity, respectively, of the liquid, ΔV and ρ_g are the velocity difference and density, respectively, of the combustion-gas stream relative to the liquid jet, and D_o is the diameter of the fuel-tube orifice.

INTRODUCTION

Experimental data have been obtained for liquid-jet atomization, in high-velocity airstreams (ref. 1) and in relatively "stable" combustion environments (ref. 2). However, little is known about the breakup mechanism for fuel jets with oscillatory or "unstable" combustion. This lack of knowledge may be a result primarily of the destructive effects of oscillatory or unstable combustion and the problem of controlling the phenomon itself in order to study it. Part of this difficultly may be attributed to the rapid rates at which heat, momentum, and mass are transferred in the presence of high-frequency and high-amplitude acoustic oscillations.

In the case of nonacoustic low-frequency fluctuations of chamber pressure, destructive effects are not severe, and data on atomization and vaporization have been obtained (ref. 2). It was shown that an increase in the fineness of the breakup of a fuel jet was accompanied by an increase in the amplitude of the chamber-pressure fluctuations approximately by a factor of four, whereas the frequency of the fluctuations was increased only a small amount, from a mean frequency of approximately 90 to 100 cps. Thus, for such conditions, only the amplitude of the chamber-pressure fluctuations appeared to be affected appreciably by the fineness of atomization.

The present investigation was conducted first to set up constant-frequency acoustic oscillations in a combustor burning ethanol and liquid oxygen and then to study the effect of the amplitude of the oscillations on the fineness of atomization of a single jet of ethanol. The first part was accomplished by mounting a siren near the exhaust-nozzle throat. The siren produced a longitudinal acoustic oscillation in the combustor of 1190±5 cps by interrupting the flow of combustion gases through the exhaust nozzle. Photomicrographs of fuel jets breaking up inside the combustor were then taken with a high-speed camera developed at the Lewis Research Center (ref. 3). Drop-size-distribution data were obtained that could then be used to determine the effect of the amplitude of the longitudinal acoustic oscillations on the fineness of atomization of the fuel jet. As a result, calculations could be made to determine the relation between the volume-number mean drop diameter D_{30}, for the spray, and the dimensionless momentum-transfer groups Wb and Re, respectively, with constant-frequency longitudinal acoustic oscillations.

SYMBOLS

b constant in equation (5)

c* characteristic exhaust velocity, cm/sec

D drop diameter, cm or μ

D_o orifice diameter, cm

D_{30} volume-number mean drop diameter, $\left(\sum nD^3 / \sum n\right)^{1/3}$, cm or μ

f frequency, cps

L_c chamber length, cm

n number of drops

P_c chamber pressure, psia

ΔP chamber-pressure fluctuations, psia

R volume-fraction of drops with diameters >D

Re Reynolds number, $D_o \Delta V/\nu$

V_a acoustic velocity in combustor, cm/sec

V_g combustion-gas velocity, cm/sec

ΔV velocity of gases relative to liquid-jet velocity, ft/sec

Wb Weber number, $\rho_g D_o (\Delta V)^2/\sigma$

x downstream distance, in.

α constant in equation (3)

γ specific heat ratio for combustion gases

μ viscosity, P

ν kinematic viscosity, cm^2/sec

ρ density, g/cu cm

σ surface tension, dynes/cm

Subscripts:

g gas

ℓ liquid

max maximum

min minimum

o orifice

Superscript:

$(\bar{\ })$ average value

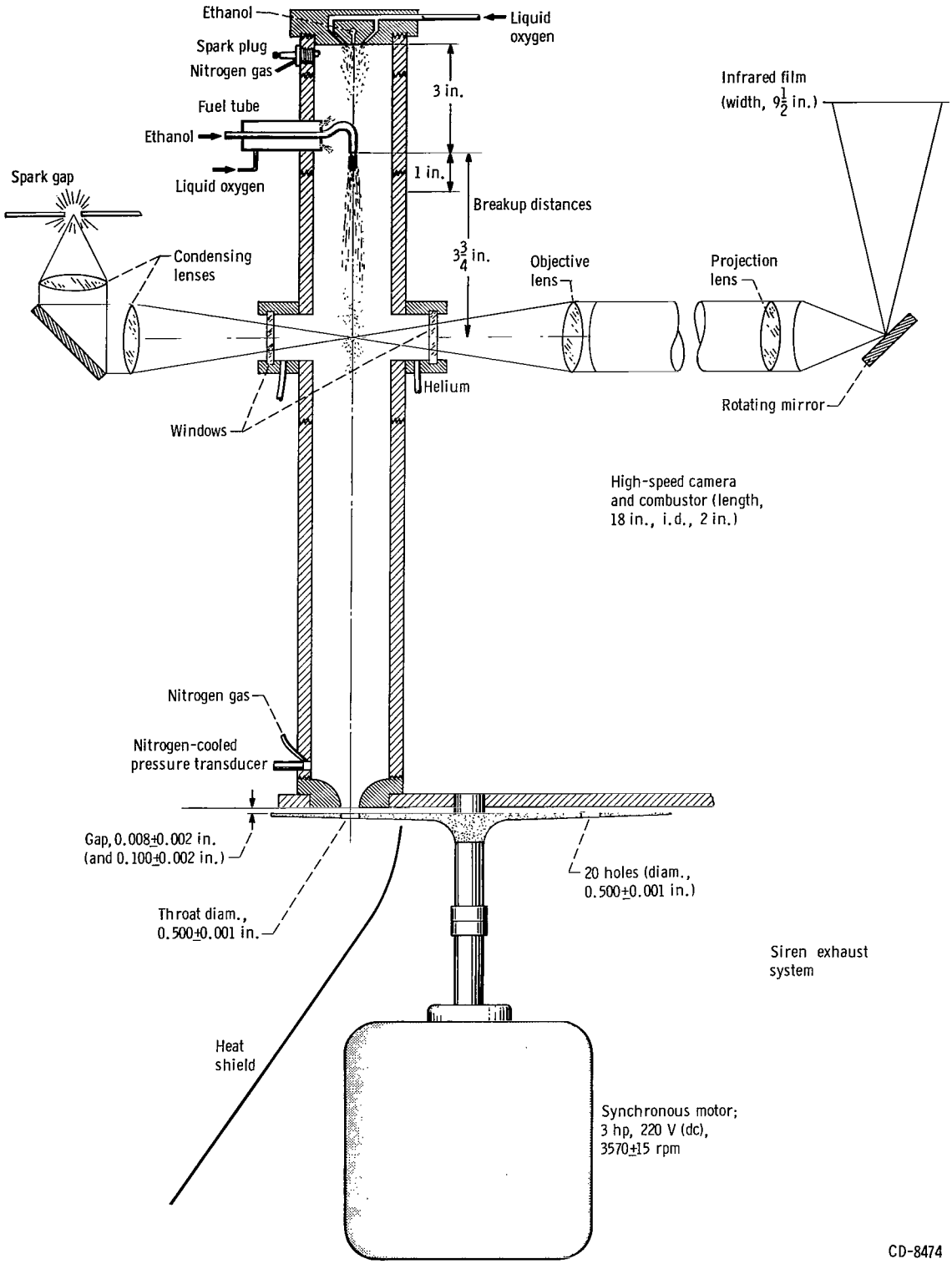

Figure 1. - Schematic diagram of experimental apparatus showing high-speed camera, rocket combustor, and siren exhaust system.

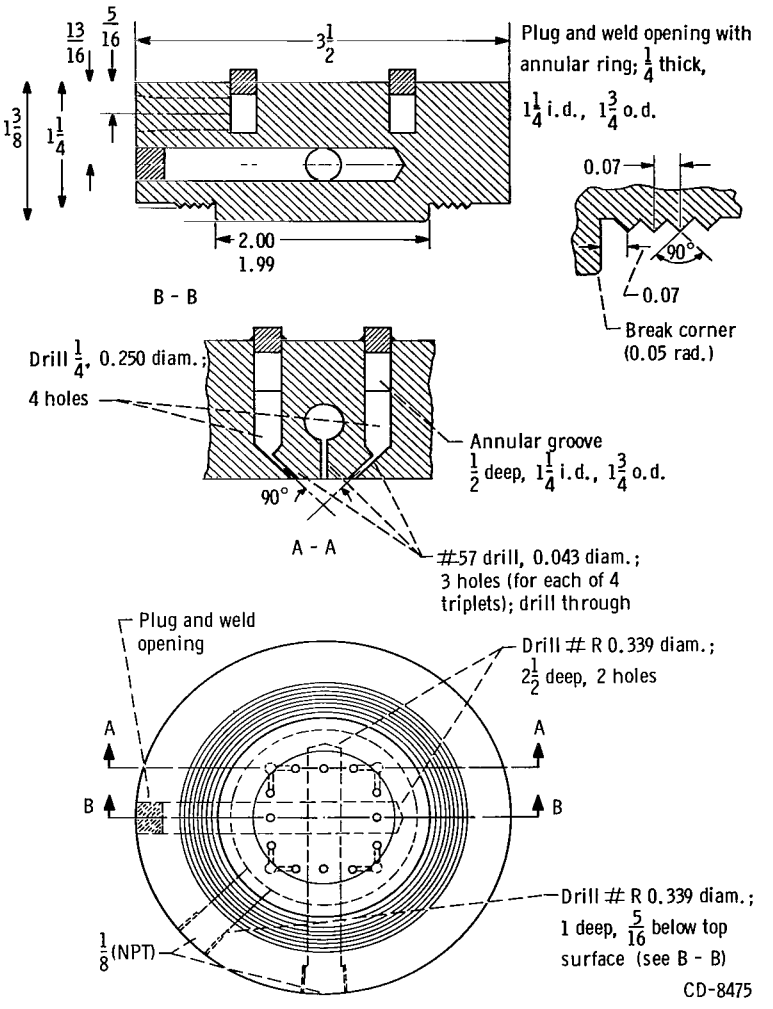

Figure 2. - Detail of rocket propellant injector. Material, 304 stainless steel, $1\frac{3}{8}$ inch thick by $3\frac{1}{2}$ inches in diameter. (All dimensions are in inches.)

APPARATUS AND PROCEDURE

The high-speed camera, the rocket combustor, the siren assembly, and the auxiliary equipment used in this study are shown in figure 1, and the details of the propellant injector are shown in figure 2. Chamber pressure was measured with a fast-response strain-gage-type pressure transducer at distances of 6 and 17 inches from the injector. A detailed description of the camera-lens system and the procedure for operating the combustor are given in reference 3.

The total weight-flow-rate of ethanol was 0.071 pound per second, with approximately 58 percent injected through the propellant injector and the remainder through the fuel tube.

Liquid oxygen was injected at a weight flow rate of 0.065 pound per second, with approximately 92 percent injected through the propellant injector and the remainder through the fuel-tube cooling jacket into the combustor, as shown in figure 1. Helium gas was injected into the chamber to cool the windows at a weight flow rate of 0.040 pound per second, and nitrogen gas, used to cool the pressure transducer, was injected at a weight flow rate of 0.060 pound per second. This gave a characteristic exhaust velocity c* of 4300 feet per second, which is approximately 93 percent of the theoretical value of c*.

The test liquid, ethanol (95 percent and 5 percent water by weight) was injected through a 0.089-inch (i.d.) fuel tube cooled with liquid oxygen and mounted inside the chamber, as shown in figure 1. The orifice of the fuel tube, 4 inches from the injector face, was positioned on the centerline of the chamber and pointed downstream toward the rocket nozzle. The distance from the fuel-tube orifice to the injector face was held constant at 3 inches. However, the distance from the fuel-tube orifice to the centerline of the camera-lens system was set at 1, 2, $3\frac{3}{4}$, 6, and 11 inches for photographing the ethanol sprays. In each case, approximately 42 percent of the ethanol burned in the combustor was injected through the fuel tube at a velocity of 16.0±0.5 feet per second.

The amplitude of the acoustic oscillations, produced by the siren at a frequency of 1190±5 cps, was controlled by adjusting the gap between the exhaust-nozzle exit and the face of the siren wheel. The gap was set at two different values, 0.008±0.002 and 0.100±0.002 inch, which gave an average chamber pressure of 180 pounds per square inch absolute and acoustic oscillations with amplitudes of 40 and 20 pounds per square inch absolute, respectively. With the siren removed completely, there were no acoustic oscillations present. Instead, a chamber pressure of 160±10 pounds per square inch absolute was obtained with random fluctuations about a mean value of approximately 90 cps, which was similar to that reported in reference 2. Thus, values of $\Delta P/P_c$ were varied from approximately zero to 0.22 by adjusting the gap between the siren wheel and the exhaust nozzle and are recorded in table I.

TABLE I. - EXPERIMENTALLY DETERMINED VALUES FOR ROCKET COMBUSTION CONDITIONS

Siren operating conditions	Pressure-amplitude ratio at 1190 cps, $\Delta P/P_c$	Average combustion gas velocity relative to liquid jet velocity, $\overline{\Delta V}$, ft/sec	Volume number mean-drop diameter, D_{30}, μ	Distance for complete breakup, x, in.
Gap, in.:				
0.008	0.22	300	62	1
0.100	0.11	150	104	4
No siren	None	90	217	6

RESULTS AND DISCUSSION

Resonant Combustion with Longitudinal Acoustic Oscillations

Resonance was established under test-firing conditions by matching the fundamental frequency of the longitudinal acoustic oscillations in the chamber with the siren frequency of 1190 cps. Thus, the combustor was acoustically represented by a cylinder closed at both ends, and the resonant frequency f may be expressed mathematically as

$$f = \frac{nV_a}{2L_c} \tag{1}$$

where $n = 1$ for the fundamental frequency, V_a is the acoustic velocity, and L_c is the chamber length, 18 inches. Transverse modes of oscillation were neglected because primarily longitudinal oscillations were produced by the siren exhaust system.

According to equation (1), an acoustic velocity of 3570 feet per second was required to obtain resonance in the chamber. This may be related to the characteristic exhaust velocity c* (ref. 4) as

$$V_a = \alpha c^* \tag{2}$$

where

$$\alpha = \gamma \left[\left(\frac{2}{\gamma + 1} \right)^{(\gamma+1)(\gamma-1)} \right]^{1/2} \tag{3}$$

and γ is the specific heat ratio.

For the conditions of this study, $\gamma = 1.37$ and $\alpha = 0.80$. The value of c* for resonant combustion was calculated from equation (2) to be 4463 feet per second. This value is within 97 percent of the theoretical value of c* of 4607 feet per second, which was calculated from equilibrium conditions in the combustor by the method given in reference 5. Agreement is good considering the fact that the preceding acoustic equations were derived for a quiescent gas of uniform temperature. Similar agreement was shown in reference 6 for a value of α of 0.72.

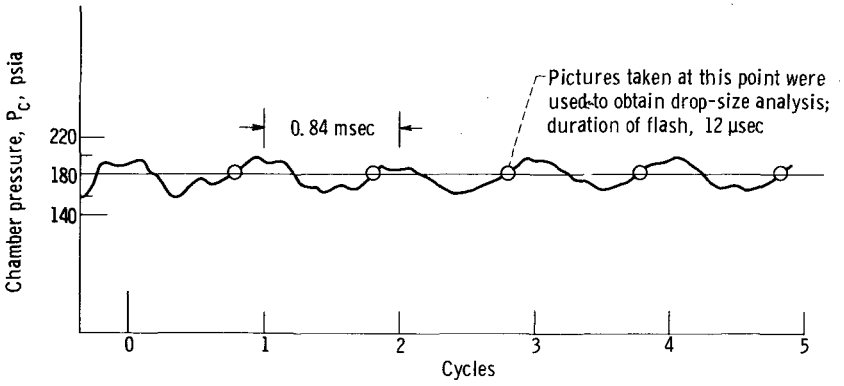

Figure 3. - Combustion-gas pressure oscillations for resonant combustion. Pressure-amplitude ratio, 0.22; frequency, 1190±5 cps; distance from exhaust nozzle, 1 inch.

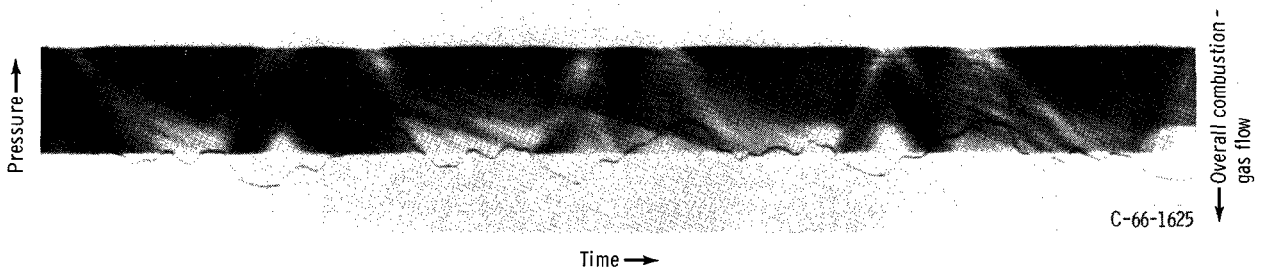

Figure 4. - Simultaneous streak photographs of combustion gases at a distance of 4 inches and chamber pressure at a distance of 6 inches from propellant injector.

Periodic Variations of Combustion-Gas Pressure and Velocity with Resonant Combustion

The variation of the combustion-gas static pressure with time at a station 17 inches downstream from the injector face is shown in figure 3. The ratio of the amplitude of the pressure oscillations to the average combustion-gas pressure $\Delta P/P_c$ was 0.22 with a gap setting of 0.008±0.002 inch between the siren wheel and the exhaust nozzle.

The streak photograph of the luminous combustion gases (fig. 4) was obtained with resonant combustion at a station 4 inches downstream from the injector face. The figure also shows the simultaneous variation of the combustion-gas pressure at a distance of 6 inches from the injector face.

The streak photograph in figure 4 shows that flow reversal occurred in the combustor under resonant combustion conditions. From the measurement of the negative and positive slopes of the streaks, the combustion-gas velocities could be determined, as shown in figure 5. The pressure trace from figure 4 is included in figure 5 for comparison. Peak negative and positive combustion-gas velocities were approximately 400 and 200 feet per second, respectively, when $\Delta P/P_c$ was 0.22. Thus, the average combustion-gas

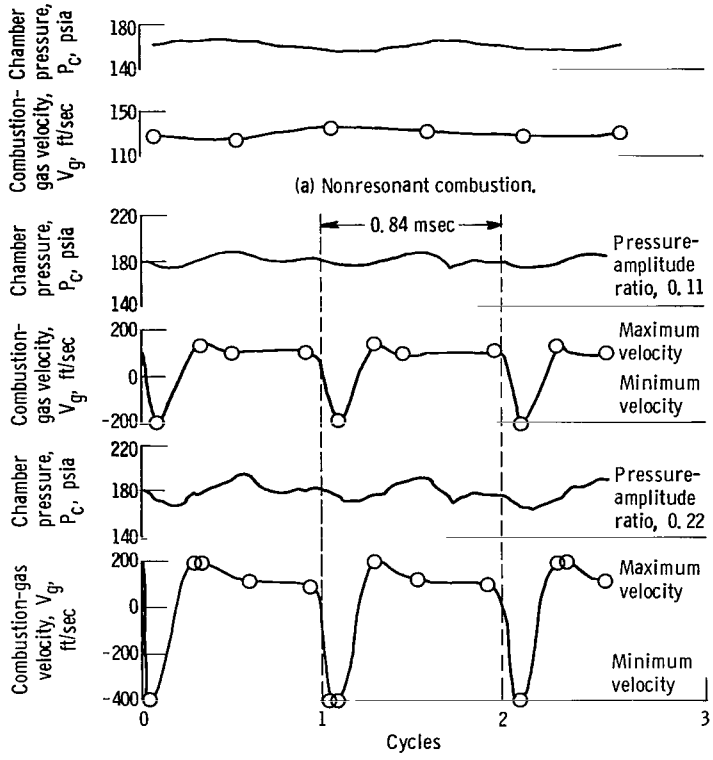

Figure 5. - Combustion-gas pressure and velocity oscillations for resonant combustion compared with nonresonant combustion conditions.

velocity relative to the liquid jet $\overline{\Delta V}$ was $1/2\left(V_{g,\,max} + V_{g,\,min}\right)$ or approximately 300 feet per second based on the peak negative and positive velocities of the combustion gases. When $\Delta P/P_c$ was 0.11, the value of $\overline{\Delta V}$ was 150 feet per second based on the same method of calculation. Values of $\overline{\Delta V}$ for resonant and nonresonant combustion conditions are given in table I.

Liquid-Jet Breakup with Siren-Induced Oscillations

When a fuel jet is injected into a rocket combustor, under resonant combustion conditions, the atomization process usually progresses through three fairly distinct stages, as illustrated in figure 6(a). In the first zone, the liquid jet appeared somewhat expanded. In the second area, it virtually appeared to be blown up into a cloud of ligaments and dense smoke. In the third or final phase, breakup was completed and the drops were accelerating in the combustion gases. The photomicrographs (figs. 6(b) to (d)) show what actually occurs in these three breakup stages in more detail.

In order to maintain continuity between pictures and obtain good reproducibility of

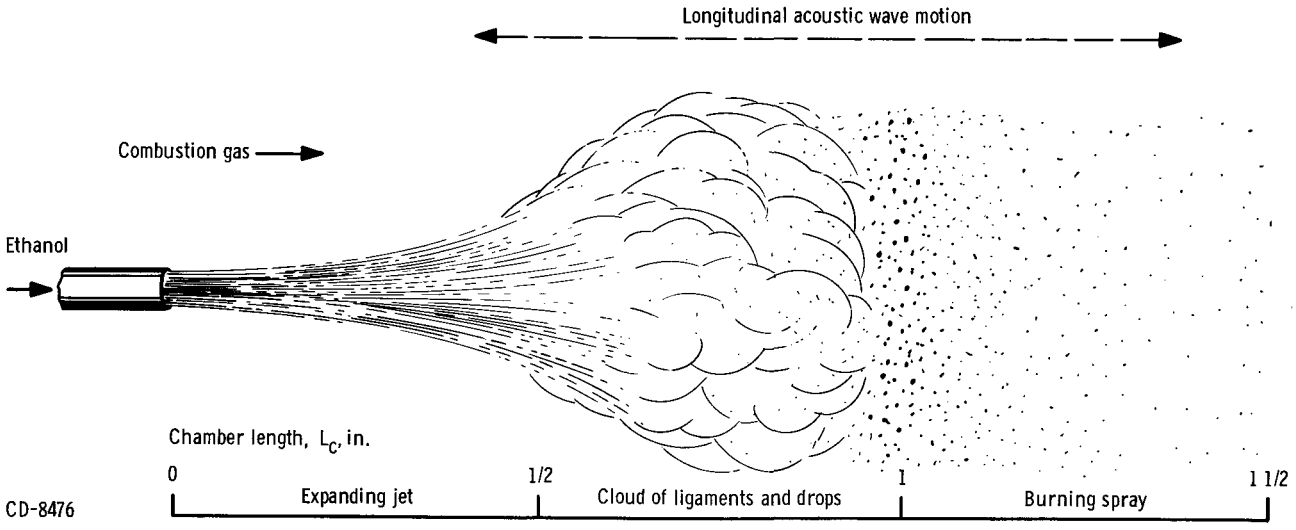

(a) Schematic representation.

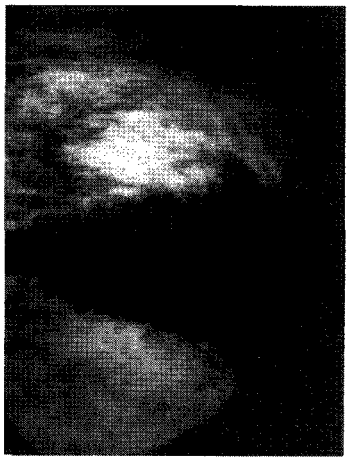

(b) Expanding jet at injector-tube orifice. X14.

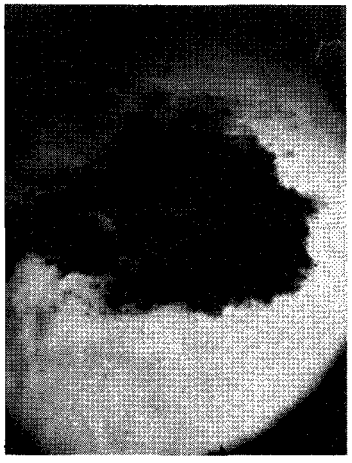

(c) Cloud of ligaments and drops 3/4 inch downstream from injector-tube orifice. X14.

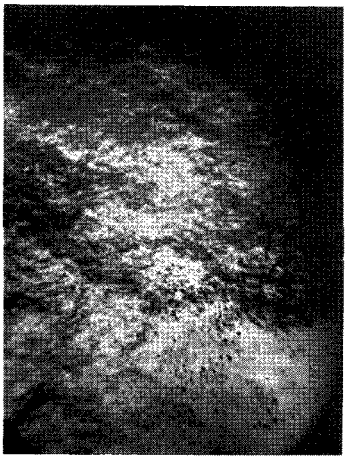

(d) Burning spray 1 inch downstream from injector-tube orifice. X14.

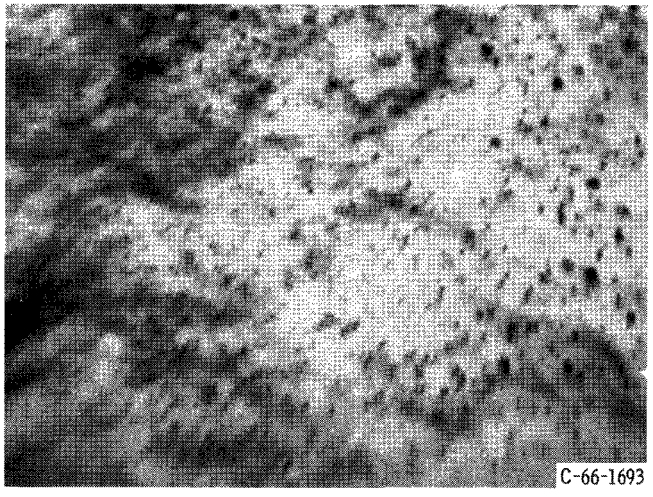

(e) Burning spray 1 inch downstream from injector-tube orifice. X28.

Figure 6. - Atomization of ethanol jet with high-frequency oscillations of combustion-gas pressure and velocity.

the drop-size data from the photomicrographs, it was necessary to take a picture precisely when the combustion-gas pressure was at the average value of 180 pounds per square inch absolute, as shown in figures 3 and 4. A photocell pickup, mounted on the camera light source, produced a signal that intersected the pressure-transducer trace on a direct-writing oscillograph. From this procedure, it could be determined whether or not the picture had been taken when the combustion-gas pressure was at its average value. However, only approximately one of five pictures was obtained in which the signal from the photocell coincided with the combustion-gas pressure at its average value in the cycle. Pictures obtained at other times in the pressure cycle were not clear due to smoke and smears produced by the acoustic wave passing through the field of view of the camera.

Drop-size-distribution data were obtained from the photomicrographs by a semiautomatic drop-size counter that gave an accuracy of ±5 microns for droplet images that were obtained at a magnification of 14. These data are recorded in table II.

Analysis of Drop-Size-Distribution Data

To characterize the automization process, a volume-number mean drop diameter D_{30} was determined for each test condition by direct integration of the drop-size data given in table II. It may be defined as follows:

$$D_{30} = \left(\frac{\sum_{D=0}^{D=D_{max}} nD^3}{\sum_{D=0}^{D=D_{max}} n} \right)^{1/3} \tag{4}$$

The Nukiyama-Tanasawa expression for size distribution

$$\frac{dR}{dD} = \frac{b^6}{120} D^5 e^{-bD} \tag{5}$$

may also be used to determine values of D_{30}; however, equation (5) can be written in the more useful form

$$\log \frac{\Delta R}{(\Delta D)D^5} = -1.7 \frac{D}{D_{30}} + \log \left[\frac{(3.915/D_{30})^6}{120} \right] \tag{6}$$

since integration of equation (5) gives $D_{30} = 3.915/b$. Then, by plotting the logarithm of $\Delta R/(\Delta D)D^5$ against D, as shown in figure 7, D_{30} may be readily determined from the slope of the straight-line plot. Values of D_{30} can also be determined by applying log-probability and Rosin-Rammler expressions for size distribution to the data (ref. 1). However, the Nukiyama-Tanasawa expression (eq. (5)) has previously been shown to

TABLE II. - DROP-SIZE-DISTRIBUTION DATA FOR COMPLETE BREAKUP

Downstream distance, x, in.					
1		$3\frac{3}{4}$		6	
Pressure-amplitude ratio, $\Delta P/P_c$					
0.22		0.11		No acoustic oscillations	
Average drop diameter, $\overline{D}$, μ	Number of drops in given drop-size increment, n	Average drop diameter, $\overline{D}$, μ	Number of drops in given drop-size increment, n	Average drop diameter, $\overline{D}$, μ	Number of drops in given drop-size increment, n
12	170	12	54	26	55
24	130	24	85	52	117
36	324	36	106	78	155
48	242	48	147	104	131
60	173	60	152	130	127
72	112	72	108	156	114
84	69	84	77	182	111
96	46	96	61	208	81
108	20	108	68	234	83
120	10	120	45	260	52
132	6	132	50	286	47
144	2	144	43	312	32
---	---	156	31	338	24
---	---	168	22	364	21
---	---	180	20	390	17
---	---	192	14	416	11
---	---	204	13	442	7
---	---	216	7	468	6
---	---	228	4	494	3
---	---	240	1	520	1
---	---	---	---	546	1
---	---	---	---	572	1

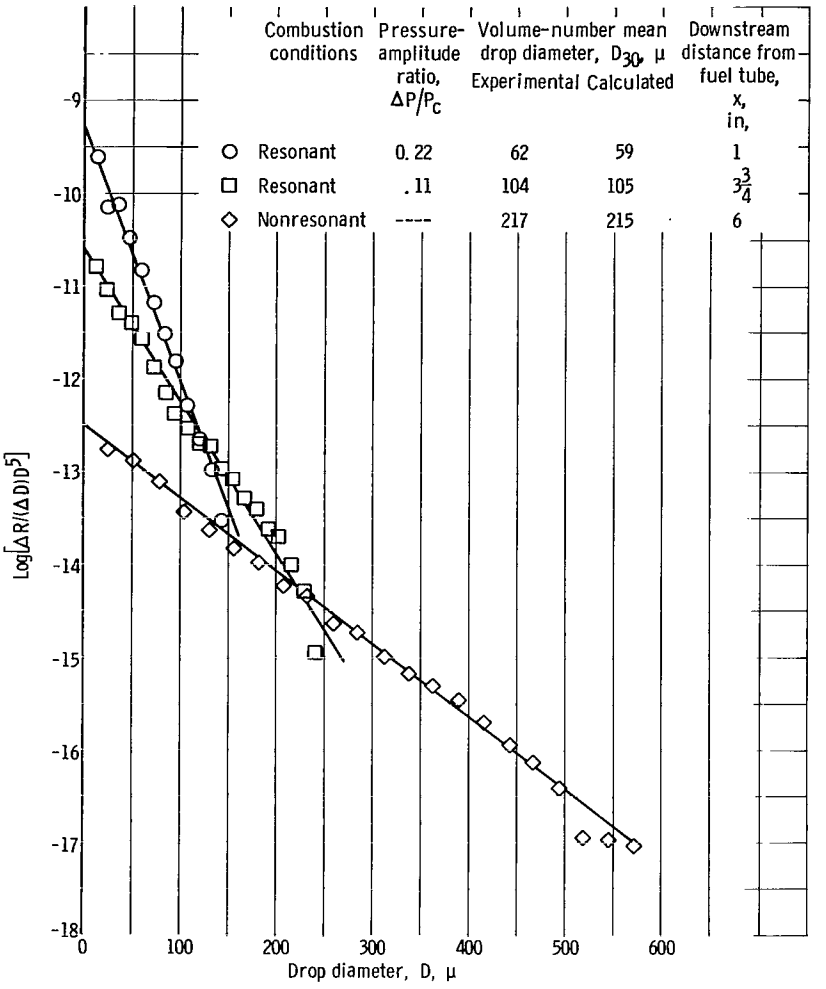

Figure 7. - Nukiyama-Tanasawa analysis for complete atomization with resonant and nonresonant combustion conditions.

describe adequately the drop-size distribution of sprays produced in rocket combustors (ref. 2). Also in figure 7, good agreement is shown between values of D_{30} determined from the Nukiyama-Tanasawa expression and those determined by direct integration of the drop-size data.

Momentum-Transfer Relations with Oscillatory Combustion

Values for D_{30} were determined at several stations downstream from the injector-tube orifice, as shown in figure 8. They indicate that atomization was much faster and that a much finer spray was produced in the presence of the 1190±5-cps acoustic oscillations. Also, the highest amplitude oscillations $\Delta P/P_c = 0.22$ produced the smallest

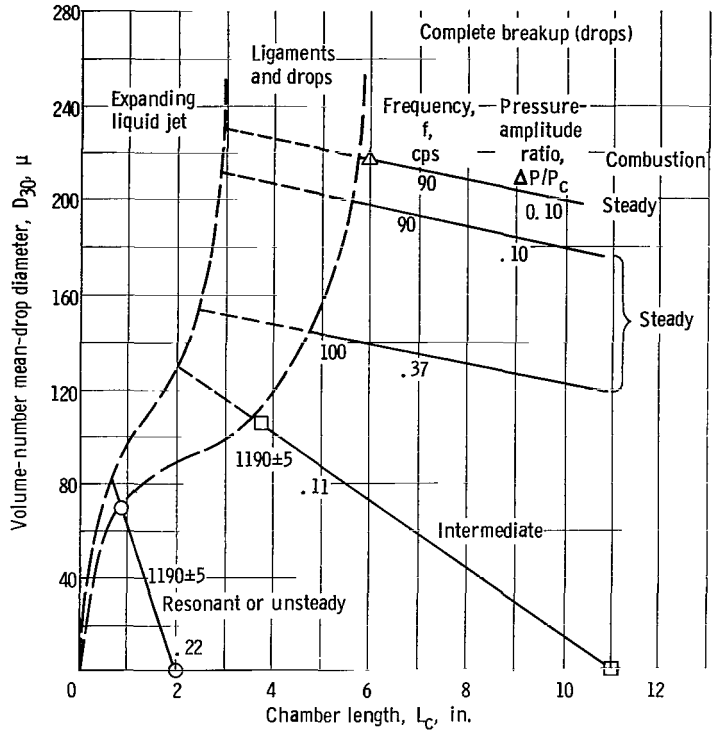

Figure 8. - Atomization of ethanol jets in a combustor.

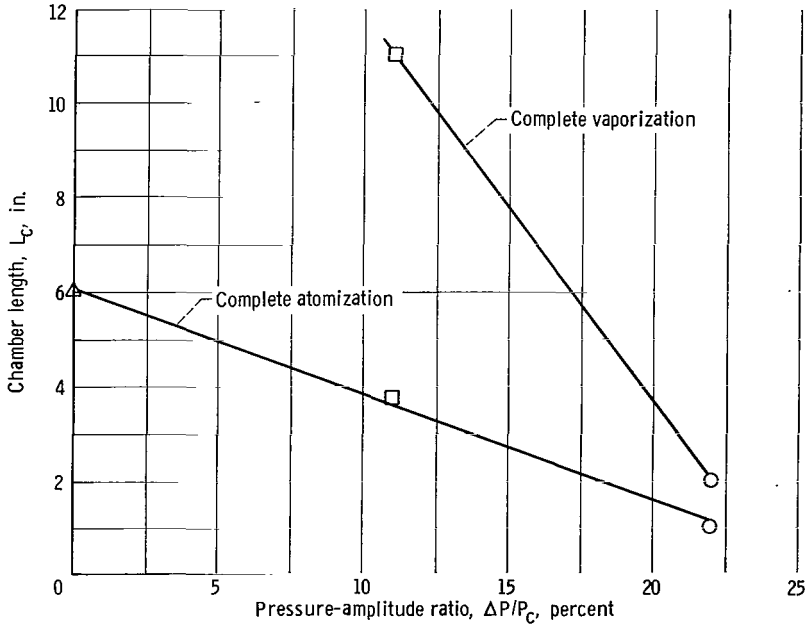

Figure 9. - Effect of amplitude of oscillations on distance required for atomization and vaporization.

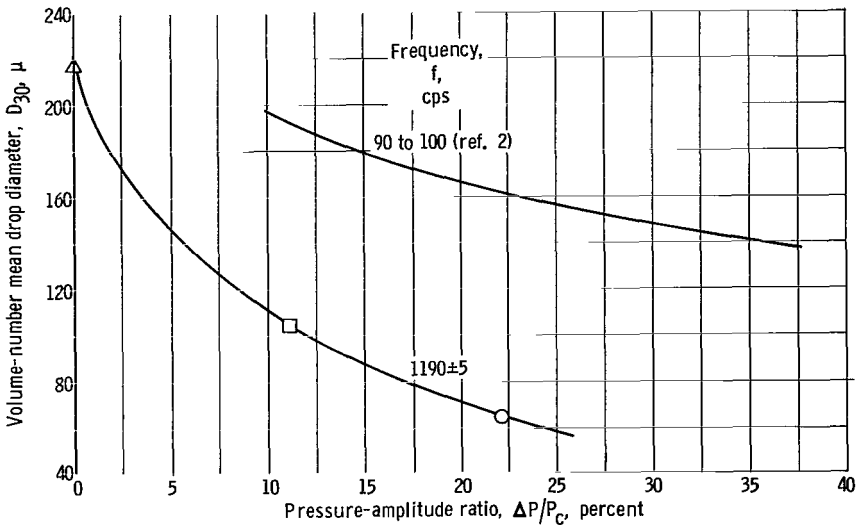

Figure 10. - Effect of amplitude of oscillations on atomization.

mean drop size D_{30} of 62 microns, and complete breakup occurred in a short distance, that is, 1 inch. In the case of "steady" combustion without the siren, a relatively coarse spray was completely formed in 6 inches. Data plots from reference 2 are also included in figure 8 to show the relatively coarse spray formed with random low-frequency chamber-pressure fluctuations present in the combustor.

Figures 9 and 10 show that the distances required for complete atomization and vaporization and the mean drop diameter D_{30} vary inversely with the pressure-amplitude ratio $\Delta P/P_c$. Data from reference 2 are also plotted in figure 10, which shows the effect of the pressure-amplitude ratio $\Delta P/P_c$ to be considerably greater for the controlled high-frequency oscillations.

In reference 1, it was shown that the velocity difference between the airstream and the liquid jet had the greatest effect on mean drop size of all the variables considered in the breakup process. As a result, the following relation was derived

$$\frac{D_{30}}{D_o} = 3.9(WbRe)^{-1/4} \tag{7}$$

where

$$Wb = \frac{\rho_g D_o (\Delta V)^2}{\sigma}$$

and

$$Re = D_o \Delta V \frac{\rho_\ell}{\mu_\ell}$$

Here, the more common definition of the Weber number is used, whereas the reciprocal Weber number was used in reference 1.

Similarly, in the present study, the velocity difference was also considered to be one of the most important factors in the atomization process. However, in the case of resonant combustion, the problem of determining the combustion-gas velocity is more difficult since it varies considerably during each cycle of the acoustic oscillation, as shown in figure 5 (p. 9). Thus, the average velocity difference for each test condition, as shown in table I, was used to calculate the product WbRe given in equation (7).

Values for Wb and Re were accordingly calculated and plotted against the ratio D_{30}/D_o, as shown in figure 11. Equation (7) and data given in reference 2 are also included for comparison. The agreement between the different methods of orienting the

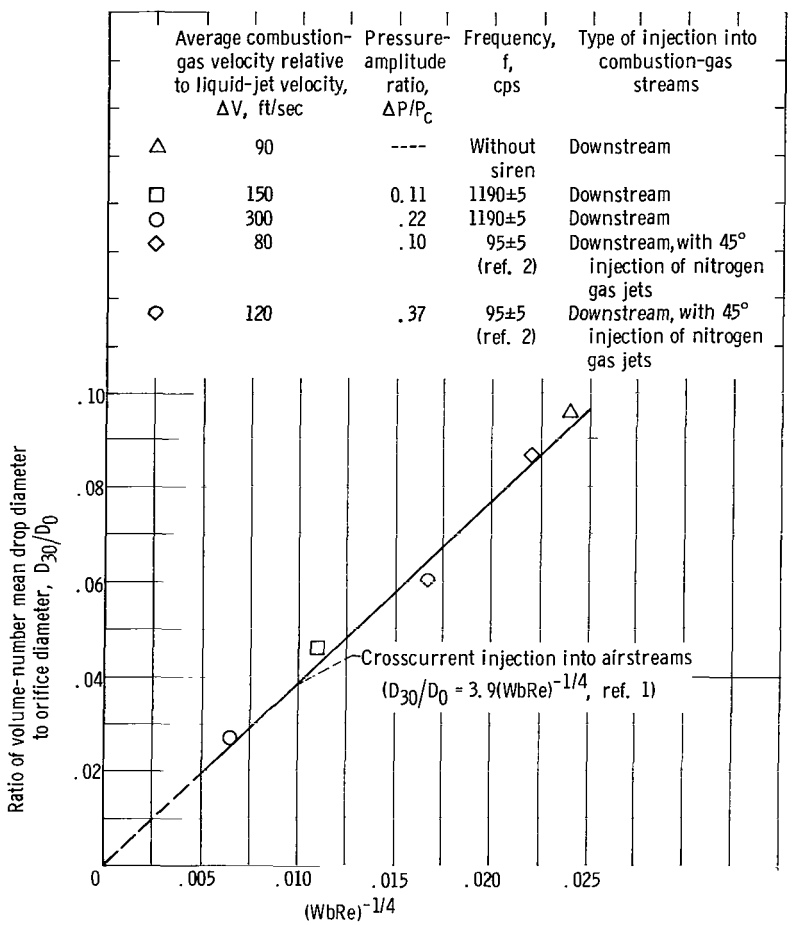

Figure 11. - Correlation of dimensionless ratio D_{30}/D_o with product of Reynolds and Weber numbers.

liquid jet with repsect to the gas stream is fairly good. The velocity of the gas stream, relative to the liquid jet, is indicated to be determinative in the breakup process with cocurrent as well as crosscurrent injection methods.

Similarly, the acoustic oscillations were effective in producing a fine spray inside the combustor. This result may be attributed to the relatively high velocity difference between the combustion gases and the liquid jet during resonant combustion.

SUMMARY OF RESULTS

The atomization of ethanol jets in oscillatory combustion-gas flow was rapid and efficient due to the high velocity of the combustion gases relative to the liquid jet. Resulting values of the volume-number mean drop diameter were correlated with the orifice diameter and the product of the Weber number and the Reynolds number. Also, this correlation agreed well with past studies on liquid-jet breakup in both airstreams and relatively steady combustion-gas flow. Thus, liquid-jet breakup in oscillatory combustion-gas flow agreed with the results from other studies of liquid-jet atomization when the velocity difference was taken as an average of the maximum negative and positive gas velocities relative to the liquid jet.

Lewis Research Center,
National Aeronautics and Space Administration,
Cleveland, Ohio, March 31, 1966.

REFERENCES

1. Ingebo, Robert D.; and Foster, Hampton H.: Drop-Size Distribution for Crosscurrent Breakup of Liquid Jets in Airstreams. NACA TN 4087, 1957

2. Ingebo, Robert D.: Vaporization Rates of Ethanol Sprays in a Combustor with Low-Frequency Fluctuations of Combustion-Gas Pressure. NASA TN D-1408, 1962.

3. Ingebo, Robert D.: Photomicrographic Tracking of Ethanol Drops in a Rocket Chamber Burning Ethanol and Liquid Oxygen. NASA TN D-290, 1960.

4. Sutton, George P.: Rocket Propulsion Elements: an Introduction to the Engineering of Rockets. Second ed., John Wiley & Sons, Inc., 1956.

5. Gordon, Sanford; Zeleznik, Frank J.; and Huff, Vearl N.: A General Method for Automatic Computation of Equilibrium Compositions and Theoretical Rocket Performance of Propellants. NASA TN D-132, 1959.

6. Tischler, Adelbert O.; Massa, Rudolph V.; and Mantler, Raymond L.: An Investigation of High-Frequency Combustion Oscillations in Liquid-Propellant Rocket Engines. NACA RM E53B27, 1953.

"The aeronautical and space activities of the United States shall be conducted so as to contribute . . . to the expansion of human knowledge of phenomena in the atmosphere and space. The Administration shall provide for the widest practicable and appropriate dissemination of information concerning its activities and the results thereof."

—NATIONAL AERONAUTICS AND SPACE ACT OF 1958

NASA SCIENTIFIC AND TECHNICAL PUBLICATIONS

TECHNICAL REPORTS: Scientific and technical information considered important, complete, and a lasting contribution to existing knowledge.

TECHNICAL NOTES: Information less broad in scope but nevertheless of importance as a contribution to existing knowledge.

TECHNICAL MEMORANDUMS: Information receiving limited distribution because of preliminary data, security classification, or other reasons.

CONTRACTOR REPORTS: Technical information generated in connection with a NASA contract or grant and released under NASA auspices.

TECHNICAL TRANSLATIONS: Information published in a foreign language considered to merit NASA distribution in English.

TECHNICAL REPRINTS: Information derived from NASA activities and initially published in the form of journal articles.

SPECIAL PUBLICATIONS: Information derived from or of value to NASA activities but not necessarily reporting the results of individual NASA-programmed scientific efforts. Publications include conference proceedings, monographs, data compilations, handbooks, sourcebooks, and special bibliographies.

Details on the availability of these publications may be obtained from:

SCIENTIFIC AND TECHNICAL INFORMATION DIVISION

NATIONAL AERONAUTICS AND SPACE ADMINISTRATION

Washington, D.C. 20546